Available online at www.sciencedirect.com

ScienceDirect

Geochimica et Cosmochimica Acta 223 (2018) 350–363

Geochimica et Cosmochimica Acta

www.elsevier.com/locate/gca

Gallium isotope fractionation during Ga adsorption on calcite and goethite

Wei Yuan [a,b], Giuseppe D. Saldi [c], JiuBin Chen [a,*], Marino Vetuschi Zuccolini [d], Jean-Louis Birck [e], Yujie Liu [a], Jacques Schott [c]

[a] State Key Laboratory of Environmental Geochemistry, Institute of Geochemistry, Chinese Academy of Sciences, Guiyang 550081, China
[b] University of Chinese Academy of Sciences, Beijing 100049, China
[c] Géoscience Environnement Toulouse, CNRS (UMP 5563)-OMP-Université Paul-Sabatier, 14, Avenue Édouard Belin, 31400 Toulouse, France
[d] Laboratorio di Geochimica at DIPTERIS, Università di Genova, Corso Europa 26, 16132 Genova, Italy
[e] Laboratoire de Geochimie et Cosmochimie, Institute de Physique du Globe de Paris (IPGP), 75252 Paris, France

Received 23 May 2017; accepted in revised form 8 December 2017; available online 16 December 2017

Abstract

Gallium (Ga) isotopic fractionation during its adsorption on calcite and goethite was investigated at 20 °C as a function of the solution pH, Ga aqueous concentration and speciation, and the solid to solution ratio. In all experiments Ga was found to be enriched in light isotopes at the solid surface with isotope fractionation $\triangle^{71}Ga_{solid\text{-}solution}$ up to −1.27‰ and −0.89‰ for calcite and goethite, respectively. Comparison of Ga isotopic data of this study with predictions for 'closed system' equilibrium and 'Rayleigh fractionation' models indicates that the experimental data are consistent with a 'closed system' equilibrium exchange between the fluid and the solid. The results of this study can be interpreted based on Ga aqueous speciation and the structure of Ga complexes formed at the solid surfaces. For calcite, Ga isotope fractionation is mainly triggered by increased Ga coordination and Ga–O bond length, which vary respectively from 4 and 1.84 Å in $Ga(OH)_4^-$ to 6 and 1.94 Å in the >Ca–O–$GaOH(OH_2)_4^+$ surface complex. For goethite, despite the formation of Ga hexa-coordinated >FeOGa$(OH)_2^0$ surface complexes (Ga–O distances of 1.96–1.98 Å) both at acid and alkaline pH, a similar extent of isotope fractionation was found at acid and alkaline pH, suggesting that $Ga(OH)_4^-$ is preferentially adsorbed on goethite for all investigated pH conditions. In addition, the observed decrease of Ga isotope fractionation magnitude observed with increasing Ga surface coverage for both calcite and goethite is likely related to the formation of Ga surface polymers and/or hydroxides with reduced Ga–O distances. This first study of Ga isotope fractionation during solid-fluid interactions suggests that the adsorption of Ga by oxides, carbonates or clay minerals could yield significant Ga isotope fractionation between secondary minerals and surficial fluids including seawater. Ga isotopes thus should help to better characterize the surficial biogeochemical cycles of gallium and its geochemical analog aluminum.

Keywords: Gallium isotopes; Significant fractionation; Adsorption; Calcite; Goethite

1. INTRODUCTION

Chemical weathering, which is caused by the interaction of water with minerals at the Earth's surface, plays an important role in continental erosion, soil formation, plant nutrient release, delivery of dissolved elements to streams and the oceans, and the control of atmospheric CO_2 concentration and climate (Berner, 1997; Galy and France-Lanord, 1999; Gaillardet et al., 1999; Hilton et al., 2011; Tipper et al., 2006; Vance et al., 2009). Among the chemical elements involved in weathering, aluminum (Al) is of

* Corresponding author.
E-mail address: chenjiubin@vip.gyig.ac.cn (J. Chen).

https://doi.org/10.1016/j.gca.2017.12.008
0016-7037/

particular interest because it is a major constituent of rock-forming minerals, especially aluminosilicates such as feldspars, micas and clay minerals. During weathering processes, Al is sorbed onto and/or incorporated into inorganic and organic colloids, and its insolubility leads to the formation of secondary solids such as clays or Al hydroxides (Hydes and Liss, 1977; Hydes, 1979, 1983; Measures and Edmond, 1988; Orians and Bruland, 1988; Pokrovsky and Schott, 2002; Shiller, 1988; Shiller and Frilot, 1996). Although characterizing Al weathering chemistry is of importance, this knowledge is still incompletely understood due to the numerous interactive processes that impact the chemical behavior of Al. Stable isotope approaches have proven useful for revealing weathering process and their interactions for other key elements such as calcium (Gussone et al., 2016; Hindshaw et al., 2011) and magnesium (Opfergelt et al., 2012; Teng et al., 2010). However, Al has only one naturally-occurring stable isotope (^{27}Al) and thus it is not possible to use Al stable isotope approaches to aid in quantifying the weathering intensity and the extent of secondary phase precipitation, or to estimate the respective fluxes of dissolved and particulate Al to the ocean. Thus, there is value in identifying and developing proxy stable isotope tracers of Al behavior during weathering to provide additional insights into past and present alteration processes involving Al that have affected the Earth's surface.

Gallium (Ga) has been considered as a potential tool to help decipher Al behavior during these alteration processes (Goldschmidt, 1954; Burton et al., 1959; Orians and Bruland, 1988; Shiller, 1988; Shiller and Frilot, 1996). Ga, located just below Al in column IIIA of the periodic table, has two stable isotopes, ^{69}Ga and ^{71}Ga, with abundances of 60.1% and 39.9%, respectively (De Laeter, 1972). Its abundance in the Earth's crust is approximately 15 ppm (Wedepohl, 1995) and it is found as a minor constituent in many minerals (Wood and Samson, 2006). Trivalent Ga is the stable oxidation state at the Earth's surface, and owing to similar ionic radii it frequently substitutes for Al^{3+} and/or Fe^{3+} in common rock-forming minerals (Gottardi et al., 1978). The high charge and small radius of Ga (0.62 Å) rank it, like Al (0.54 Å), among the "hard" acids according to the classification of Pearson (1963), thus implying that these cations tend to form solute complexes with hard donor atoms such as hydroxyls, carboxylates or phenolates.

Both Al^{3+} and Ga^{3+} undergo strong hydrolysis as fluid pH increases with the formation of hydroxide complexes (successively $Al,GaOH^{2+}$, $Al,Ga(OH)_2^+$, $Al,Ga(OH)_3^0$ and $Al,Ga(OH)_4^-$) although the extent of Ga hydrolysis is more marked. For example, at 25 °C and pH = 6, Al aqueous speciation is dominated by $Al(OH)_3^0$ and $Al(OH)_2^+$ whereas Ga is exclusively present as $Ga(OH)_4^-$ (Benézéth et al., 1997; Tagirov and Schott, 2001). The more effective hydrolysis of aqueous Ga compared to that of aqueous Al at given temperature and pH has been invoked to account for both the lower reactivity of Ga (longer residence time) than Al in the oceans, due to its presence as the more "soluble" gallate complex (Orians and Bruland, 1988) and the higher mobility of Al in streams as a result of the stronger complexation with organic matter of the less hydrolyzed Al species (Martell and Hancock, 2013). This led Shiller and Frilot (1996) to propose the use of dissolved Ga concentration measurements for estimating the mobilization of Al in watersheds by inorganic or organic complexation processes for which the weathering regimes are known.

Advances over the last decade in multiple-collector inductively coupled plasma-source mass spectrometry (MC-ICP-MS), combined with the recent development of chemical purification methods that allow for accurate measurement of Ga isotopes ratios (Yuan et al., 2016; Zhang et al., 2016; Kato et al., 2017), offer new possibilities for the use of Ga and its isotopes to decipher the weathering mechanisms and the behavior of Al in continental surficial waters and in the oceans. Ga isotopes appear to be a new promising tool in this regard, because (i) large variations of δ^{71}Ga (see Eq. (1) for definition of the delta terminology) up to 1.83‰ have already been detected in various standard samples (Yuan et al., 2016; Zhang et al., 2016; Kato et al., 2017), and (ii) the coordination change that Ga undergoes, from 4 in solution (pH $\geq$ 5, Benézéth et al., 1997) to 6 at the surface or in the crystal structure of oxides and carbonates (Pokrovsky et al., 2004; Persson et al., 2006), is likely to induce significant isotope fractionation as a result of the increase of the metal-oxygen bond length (Criss, 1999; Schauble, 2004; Schott et al., 2016).

Adsorption on oxides, clays, carbonates, and inorganic and organic colloids is known to be an important process in the control of trivalent elements like Ga in surficial environments and their scavenging from natural waters (Pokrovski et al., 2002; Gaillardet et al., 2003; Pokrovsky et al., 2004, 2006). The structure of the complexes formed by Ga at the surface of carbonates (calcite, magnesite) and oxides (birnessite, goethite) has recently been characterized using X-ray Absorption Spectroscopy (Pokrovsky et al., 2004; Persson et al., 2006). The present study extends this knowledge to Ga isotope fractionation during Ga adsorption on calcite and goethite. It is expected that this work will allow identification and quantification of the physico-chemical parameters controlling Ga isotope behavior in the presence of Fe hydrous oxides and carbonates, and provide the first constraints on the extent of Ga isotope fractionation in aquatic environments at the Earth's surface.

2. MATERIALS AND METHODS

2.1. Starting materials

Synthetic calcite and goethite were used for the adsorption experiments. Calcite powder with sub-micrometer crystal size was obtained by precipitation from supersaturated solutions of $(NH_4)_2CO_3$ and $CaCl_2$ at pH $\sim$ 10. The goethite powder (aggregates of crystals having an average size of 0.1 μm, as determined by laser diffraction technique) was synthesized in the LEM laboratory (Nancy University, France) following a procedure described by Cornell and Schwertmann (2004) and based on the oxidative hydrolysis of $FeSO_4$. Both powders were from the same batches previously characterized by Pokrovsky et al. (2004, 2006) to investigate Ga and Ge adsorption on calcite and goethite,

respectively. Supplementary X-ray diffraction analyses provided verification of their crystallinity and the absence of other phases. Trace element analysis of studied solids performed by ICP-MS did not detect any impurities in amounts ≥ 0.1 wt%, and Ga content was below 1 ppm. The specific surface area of calcite and goethite was 18.6 m^2/g and 23.2 m^2/g, respectively, as determined by the B. E.T. nitrogen adsorption technique.

For the Ga adsorption experiments, a 1000 ppm Ga^{3+} stock solution was prepared by dissolving Ga (III) nitrate hydrate (Puratronic®, 99.999%, by Alfa Aesar) in ultrapure water (18.2 MΩ cm) and adjusting the pH to 1.5 by addition of HNO_3. From this stock solution, other solutions of lower Ga concentrations (1–10 ppm) at near-neutral pH were prepared. These solutions were freshly made each time before starting the experimental runs and added immediately to calcite and goethite suspensions, in order to prevent any possible precipitation of Ga oxyhydroxide before use.

All labware (Teflon vials, pipette tips and storage bottles, etc.) was carefully cleaned in an ultra-clean room following an established procedure that entails the use of EXTRANS solution, a mixture of concentrated HCl and HNO_3, HF, and 1 M HCl and repeated washing with ultrapure water.

2.2. Adsorption experiments

The adsorption experiments were carried out at the GET laboratory in Toulouse, France. Both series of experiments on calcite and goethite were conducted at 20 °C in 50 ml polypropylene centrifuge tubes containing a 0.01 M NaCl aqueous solution prepared with analytical grade NaCl.

To study Ga adsorption on calcite, 180 mL of a 0.01 M NaCl solution initially at equilibrium with the atmosphere was first allowed to equilibrate with 1 g of calcite powder in a polypropylene bottle. The bottle with the suspension was kept sealed and continuously shaken for the following 24 h in a thermostatic bath at 20 °C before adding any amount of HCl or NaOH to obtain the desired titration pH value. After the addition of acid/base, the solution was allowed to equilibrate with the calcite powder for another 2–3 days while regularly measuring the pH, and adding supplementary amounts of acid or base if necessary, until a constant pH value was observed. Measurements of pH, Ca concentration and alkalinity after 2–3 days showed that the solution was in equilibrium with calcite. Each solution was subsequently filtered through a 0.22 μm PTFE membranes into centrifuge tubes where a desired mass of calcite and fresh neutral Ga solution was then added successively. The centrifuge tubes were installed on a tube-rotator turning at a speed of about 20 rpm and mixed for at least 3 days. pH and Ca concentration measured at the end of the sorption runs were not found to change compared to their initial values. Ga adsorption onto the calcite surface was studied within the 7.4–8.6 pH range for different solid/aqueous solution ratios (3.6–40.3 g/l). The initial Ga concentration was fixed at 100 ppb, except for one experiment (C-11) in which the starting Ga concentration was 50 ppb.

For the batch adsorption experiments on goethite, the equilibration step between solution and sorbent was not necessary because of the very low solubility of goethite. In this case Ga was directly added to the goethite suspension without any preliminary processing. The initial Ga concentration varied between 0.1 and 58.6 ppm for a solid/-solution ratio ranging from 0.1 to 10.3 g/l and $2.5 \leq pH \leq 10.5$. Typical exposure time was about 1 week. We note that the Ga concentration of several experiments was above the predicted saturation with respect to α-GaOOH (cf. Benézéth et al., 1997). However, these concentrations were much lower than those used by Persson et al. (2006) to study Ga adsorption on goethite within the same pH range. These authors did not observe any formation of Ga precipitate from their solutions and showed that the measured changes in Ga concentration were the consequence of the strong adsorption of Ga on the goethite surface. At the end of the experiments, the aqueous solution from each experiment was sampled for chemical and isotopic analyses. The sampling was carried out with 10 ml polypropylene syringes by filtering the collected volume of solution with 0.22 μm PTFE filters. The filtrate was acidified with HNO_3 and stored in a refrigerator until analysis.

2.3. pH measurements and chemical analyses

The pH of the aqueous solution was carefully measured immediately after sampling on a non-filtered volume of the solution using a Metrohm pH microelectrode and a Metrohm 913 pH-meter with an accuracy of ±0.01 units. Ca and Fe concentrations were measured by flame atomic absorption (AAS 400, Perkin-Elmer) with an uncertainty of ±1% and a detection limit of 0.02 ppm, whereas Ga was analyzed by ICP-MS (Elan 6000, Perkin-Elmer) with an uncertainty less than 5% and a detection limit of 0.01 ppb.

2.4. Ga isotope analyses

Before isotopic analyses, Ga was purified from liquid samples using a two-stage ion exchange chromatography procedure on AG 1-X4 (Bio-rad) anion exchange resin and Ln spec (TrisKem) cation exchange resin using the protocol of Yuan et al. (2016). Briefly, prior to separation, acidified solutions (HNO_3, $pH \sim 1.5$) containing at least 200 ng of Ga were evaporated to dryness at 100 °C on a hot plate and re-dissolved in ≥1 ml of 6 M HCl. Then, Ga was separated from other matrix elements using two chromatographic columns loaded with AG I-X4 and Ln-spec resin, respectively (see supporting information SI for the detailed description of the purification). Finally, the eluent containing only Ga recovered following separation of other elements was evaporated to dryness and the residual was dissolved in 2% HNO_3 for Ga isotope and concentration measurements on MC-ICP-MS and ICP-MS, respectively.

Most isotopic measurements were performed on a Neptune Plus MC-ICP-MS (Thermo Finnigan, Germany) at the Institute de Physique du Globe de Paris (IPGP, France), while a few were performed on a Nu Plasma MC-ICP-MS

(Nu Instruments Ltd., UK) at the Institute of Geochemistry, Chinese Academy of Sciences (IGCAS, Guiyang, China). The MC-ICP-MS operating conditions are described in detail in Yuan et al. (2016) and summarized in the supporting information SI. Standards and samples were introduced by Ar flux into the plasma, with Ga concentrations of about 20 μg/L and 50 μg/L in 2% HNO_3 for the Neptune Plus and Nu Plasma MC-ICP-MS, respectively. In this study, the sample-standard bracketing (SSB) method was employed to correct the mass bias for all measurements (e.g., Mason et al., 2004). Ga isotope results were expressed as $\delta^{71}Ga$, in units of per mil (‰):

$$\delta^{71}Ga = [(^{71}Ga/^{69}Ga)_{sample}/(^{71}Ga/^{69}Ga)_{NIST} - 1] \times 1000 \quad (1)$$

where the subscript NIST defines the NIST SRM 994 Ga standard (Yang and Meija, 2010). The 2SD (standard deviations) of $\delta^{71}Ga$ were calculated based on multiple measurements of each solution and was generally lower than 0.05‰.

All isotopic measurements of this study were performed on the aqueous solutions after filtration because of the much higher sensitivity of solutions to the minor changes in isotopic composition compared to the bulk solid. Assuming that the loss of Ga from the solution is solely accounted for by Ga adsorption on the calcite or goethite surface and that the solids themselves are Ga-free, the isotope ratio of adsorbed Ga ($\delta^{71}Ga_{solid}$) can be calculated from the mass balance equation using the isotope ratio in the aqueous phase ($\delta^{71}Ga_{solution}$), the fraction of Ga removed from the solution (F, % of initial amount), and the isotope ratio of the initial solution used for the experiment ($\delta^{71}Ga_{initial}$):

$$\delta^{71}Ga_{solid} = [100 \times \delta^{71}Ga_{initial} - (100 - F) \times \delta^{71}Ga_{solution}]/F \quad (2)$$

A similar approach to calculate the isotopic composition of adsorbed elements was used for Mo (Barling and Anbar, 2004), B (Lemarchand et al., 2005, 2007), Cu and Zn (Balistrieri et al., 2008), Si (Delstanche et al., 2009; Oelze et al., 2014), and Ge (Pokrovsky et al., 2014). In using Eq. (2) we carefully verified the absence of experimental artifacts due to sample handling and particularly filtration, which could possibly invalidate the results of the calculation. It was found that filtration did not change the $\delta^{71}Ga$ value of the filtrate compared to the initial Ga stock solution within the uncertainty of measurements (±0.05‰, 2SD).

The difference in the isotopic composition of Ga adsorbed on the solid and Ga in solution, $\triangle^{71}Ga_{solid\text{-}solution}$, was calculated as:

$$\Delta^{71}Ga_{solid\text{-}solution} = \delta^{71}Ga_{solid} - \delta^{71}Ga_{solution} \quad (3)$$

Note that if complete isotopic exchange between the solid and the solution occurs during Ga adsorption on the solid surface (commonly referred as *closed system equilibrium*) $\triangle^{71}Ga_{solid\text{-}solution}$ represents Ga equilibrium fractionation and is independent of the fraction F of Ga removed from the solution. In the case of irreversible Ga adsorption, on the contrary, adsorbed Ga does not continuously exchange with the solution and Rayleigh fractionation (Rayleigh, 1902) may best describe the change in $\delta^{71}Ga_{solution}$ as a function of F.

The estimated uncertainties on the calculated $\triangle^{71}Ga_{solid\text{-}solution}$ stem from (i) the uncertainty on the calculated F value, and (ii) the analytical uncertainty on the isotopic composition of the initial Ga solution and Ga isotopic ratio of each individual experiment.

2.5. Thermodynamic calculations and Ga sorption modeling

The distribution of species in solution and at the surface of calcite and goethite were modeled for each experiment using the code Visual MINTEQ v 3.1 (Gustafsson, 2012). The activity coefficients of dissolved aqueous species were calculated using the Davies equation whereas the activity coefficients of surface species were assumed to be equal to 1. Dissolved inorganic carbon (DIC) concentrations and corresponding CO_2 partial pressures (pCO_2) for calcite adsorption experiments were obtained from measured pH's and Ca concentrations assuming thermodynamic equilibrium between aqueous solution and calcite. Ga aqueous speciation was calculated using the Ga hydrolysis constants reported by Benézéth et al. (1997), which were incorporated into the Visual MINTEQ thermodynamic database.

Ga adsorption on calcite was modeled using the surface complexation model established by Pokrovsky and Schott (2002), which builds on the detailed characterization of the calcite surface chemistry gained from the spectroscopic investigation and measurements of the charge and potential of the mineral/water interface (Van Cappellen et al., 1993; Pokrovsky et al., 1999, 2000). According to this model, two primary hydration sites, $>CaOH^0$ and $>CO_3H^0$, exist at the calcite surface, having a 1:1 stoichiometry. Successive protonation/deprotonation of these sites and reactions with calcite constituent ions (Ca^{2+} and CO_3^{2-}) lead to the formation of the following surface species: $>CaOH_2^+$, $>CaO^-$, $>CaHCO_3^0$, $>CaCO_3^-$, $>CO_3^-$ and $>CO_3Ca^+$. The values of the formation constants of these species, the electrical double-layer (EDL) capacitance as well as the calcite surface site densities used in this study are listed in Table 1. Ga was assumed to adsorb as a six-coordinated anion on single protonated Ca-sites, in agreement with the X-ray absorption fine structure (XAFS) characterization of local Ga structure at the calcite surface (Pokrovsky et al., 2004). Expressed in terms of basis species of the thermodynamic database, Ga adsorption at the calcite surface can be described as:

$$>CaOH^0 + Ga^{3+} + 5H_2O \rightarrow >Ca\text{–}O\text{–}GaOH(OH_2)_4^+ + 2H^+ \quad (4)$$

The determination of the intrinsic stability constant of reaction (4) was achieved by a fitting procedure in which this constant was the only adjustable parameter, while the constants of all other surface reactions, the EDL capacitance, and the densities of surface sites were maintained constant (Table 1). An optimized value of the Ga adsorption

Table 1
Surface complexation reactions describing Ga adsorption on calcite with the corresponding intrinsic stability constants taken from Pokrovsky and Schott (2002) (reactions (1)–(6)) and determined in this study (reactions (7) and (8). The values of the other parameters defining the SCM of our system are as follows: EDL capacitance = 17 F/m^2; surface site density = 8.22 μmol/m^2.

Surface reaction	log K^0_{int} (25 °C, $I = 0$)
1. $>CO_3H^0 = >CO_3^- + H^+$	–5.1
2. $>CO_3H^0 + Ca^{2+} = >CO_3Ca^+ + H^+$	–1.7
3. $>CaOH^0 = >CaO^- + H^+$	–12.0
4. $>CaOH^0 + H^+ = CaOH_2^+$	11.85
5. $>CaOH^0 + CO_3^{2-} + 2H^+ = >CaHCO_3^0 + H_2O$	23.50
6. $>CaOH^0 + CO_3^{2-} + H^+ = >CaCO_3^- + H_2O$	17.1
7. $>CaOH^0 + Ga^{3+} + 5H_2O = Ca\text{-}H_9GaO_6^+ + 2H^+$	6.70 ± 0.1
8. $>CaOH_2^+ + Ga(OH)_4^- + 2H_2O = Ca\text{-}H_9GaO_6^+ + OH^-$	–3.49

constant (K_4) was obtained by sequential modeling of the experimental results with PEST (Doherty, 2010).

The adsorption of Ga at the goethite surface was described by a 2-pK constant capacitance model that has been adopted by many authors to describe the adsorption of different aqueous species at the surface of this mineral (e.g. Lövgren et al., 1990; Nilsson et al., 1992; Lumsdon and Evans, 1994; Pokrovsky et al., 2006). The values of goethite surface acidity constants, taken from Lövgren et al. (1990), are reported in Table 2 along with other parameters defining the surface complexation model used in the present study. In agreement with the XAFS characterization of Ga species adsorbed at the goethite surface and the surface complexation model of Persson et al. (2006), we assumed that Ga formed a six-coordinated inner-sphere mononuclear complex during the reaction of gallium with goethite surface according to the following reaction involving the aqueous and surface basis species:

$$> FeOH^0 + Ga^{3+} + 2H_2O \rightarrow > FeOGa(OH)_2^0 + 3H^+ \quad (5)$$

As for calcite, the constant value of reaction (5) was obtained by modeling our experimental results using Visual MINTEQ in combination with PEST. In this case, the density of goethite surface functional groups was fixed at 1.68 nm^{-2}, which corresponds to the density of hydroxyl groups experimentally determined by Lövgren et al. (1990), while the capacitance of the electric double layer was kept at the constant value of 0.75 F/m^2. These values are consistent with the site densities derived from crystallographic data (cf. Barrón and Torrent, 1996; Pivovarov, 1997) and the range of capacitance values commonly used for studying goethite surface complexation (Lumsdon and Evans, 1994; Cornell and Schwertmann, 2004).

3. RESULTS

3.1. Ga adsorption and its modeling

3.1.1. Calcite

Ga adsorption results are listed in Table 3. It can be seen that the measured fraction of Ga adsorbed on calcite decreases with increasing pH, from 41.1% at pH = 7.5 to 9.5% at pH = 8.5. Table 3 also lists for each experiment the values of dissolved inorganic carbon (DIC) concentration and the corresponding CO_2 partial pressures derived from measured pH and Ca concentration and the fraction of adsorbed Ga as calculated by modeling of the experimental data. The calculated fractions of Ga adsorbed were obtained for a best-fit log K_4 value of 6.7 ± 0.1, in good agreement with the estimates of Pokrovsky et al. (2004), who determined a value of 7.0 ± 0.3 for the same reaction constant involving the basis species of the thermodynamic database.

Since in the range of investigated pH the dominant calcium surface species is $>CaOH_2^+$ (cf. Pokrovsky et al., 2000), whereas $Ga(OH)_4^-$ dominates the Ga aqueous speciation (Benézéth et al., 1997), the adsorption of this element at the calcite/water interface can be expressed as:

$$> CaOH_2^+ + Ga(OH)_4^- + 2H_2O \rightarrow > Ca\text{–}O\text{–}GaOH(OH_2)_4^+ + OH^- \quad (6)$$

Table 2
Surface complexation reactions used to model Ga adsorption on goethite. Intrinsic goethite surface acidity constants (reactions (1) and (2)) are taken from Lövgren et al. (1990) whereas the intrinsic constants of formation of the Ga-complex (reactions (3)–(5)) were determined in this study. EDL capacitance = 0.75 F/m^2; surface site density = 1.68 nm^{-2} (2.79 μmol/m^2).

Goethite surface reactions	log K^0_{int} (25 °C. $I = 0$)
1. $>FeOH^0 + H^+ = >FeOH_2^+$	7.47
2. $>FeOH^0 = >FeO^- + H^+$	–9.51
3. $>FeOH^0 + Ga^{3+} + 2H_2O = >FeOGa(OH)_2^0 + 3H^+$	–1.05 ± 0.2
4. $>FeOH_2^+ + Ga^{3+} + 2H_2O \rightarrow >FeOGa(OH)_2^0 + 4H^+$	–8.52
5. $>FeOH_2^+ + Ga(OH)_4^- \rightarrow >FeOGa(OH)_2^0 + 2H_2O$	7.14

Table 3
Summary of the Ga adsorption experiments on calcite with the corresponding pH, solid to aqueous solution ratios (Cc/Vol) and the relative concentrations of Ca, dissolved inorganic carbon (DIC) and calculated pCO_2. All experiments were conducted at the constant electrolyte (NaCl) concentration of 0.01 M. Note that total dissolved carbon and corresponding pCO_2 were calculated on the basis of measured Ca concentrations and pH's assuming thermodynamic equilibrium with calcite. The table also lists the Ga aqueous concentration measured before and after each experiment, the surface density of Ga adsorbed, and the comparison between measured and modeled percentage of Ga adsorbed (last two columns).

Sample No.	pH	Cc/Vol	[Ca]	DIC	log pCO_2	$[Ga]_{in}$	$[Ga]_{fin}$	$[Ga]_{tot}$	$[Ga]_{ads}$	% Ga adsorbed	
		g/l	mM	mM		ppb	ppb	nmol/m^2	nmol/m^2	Measured	Model
C-1	7.4	3.6	3.13	1.84	−2.41	107.5	80.1	22.8	5.8	25.5	25.8
C-2	7.4	3.6	3.03	1.90	−2.40	107.5	79.9	22.7	5.8	25.7	25.8
C-3	7.5	3.6	3.58	1.29	−2.67	106.7	74.4	22.9	6.9	30.3	22.0
C-4	7.5	3.7	2.79	1.60	−2.57	103.3	68.2	21.8	7.4	34.0	22.1
C-5	7.5	8.1	3.28	1.39	−2.63	106.6	62.8	10.2	4.2	41.1	38.6
C-6	8.0	6.7	1.24	1.01	−3.24	105.3	88.3	12.1	1.9	16.1	13.3
C-7	8.1	25.1	0.98	1.01	−3.34	105.7	81.6	3.2	0.7	22.8	31.0
C-8	8.2	40.2	0.83	0.93	−3.47	106.5	78.6	2.0	0.5	26.2	36.0
C-9	8.5	10.1	0.68	0.57	−3.99	105.6	95.6	8.1	0.8	9.5	6.5
C-10	8.6	40.1	0.48	0.63	−4.04	106.4	90.0	2.0	0.3	15.4	17.5
C-11	8.6	40.3	0.51	0.61	−4.06	53.4	44.8	1.0	0.2	16.1	17.6

The stability constant of reaction (6) can be deduced from the value of K_4, the Ga hydrolysis constants and the formation constant of $>CaOH_2^+$ at the calcite surface (see Table 1). Taking into account the values of these constants, the derived value of log K_6 is equal to −3.49. A comparison between the experimental values of adsorbed Ga and those predicted by the surface complexation model using the determined value of K_4 is provided in Fig. 1. It can be seen that a satisfactory agreement is obtained, the difference between measured and predicted values being of 8–12% for 4 samples but lower than 3% for all the others (see Table 3). In Fig. 2 the adsorbed Ga concentration

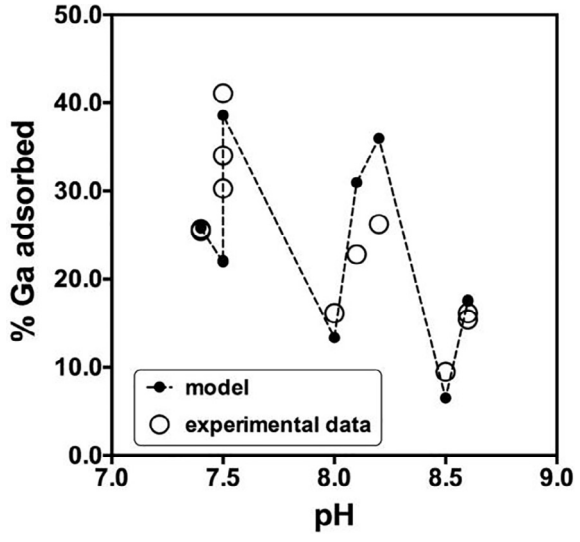

Fig. 1. Comparison between the measured percentages of adsorbed Ga on calcite (empty circles) and those predicted by the SCM (black dots connected by the dashed line). Note that the experiments were conducted with solid/fluid ratios varying between 3.6 and 40.3 g/l. Initial Ga concentrations were of 100 ppb except for run C-11 (Ga_0 = 50 ppb; cf. Table 3).

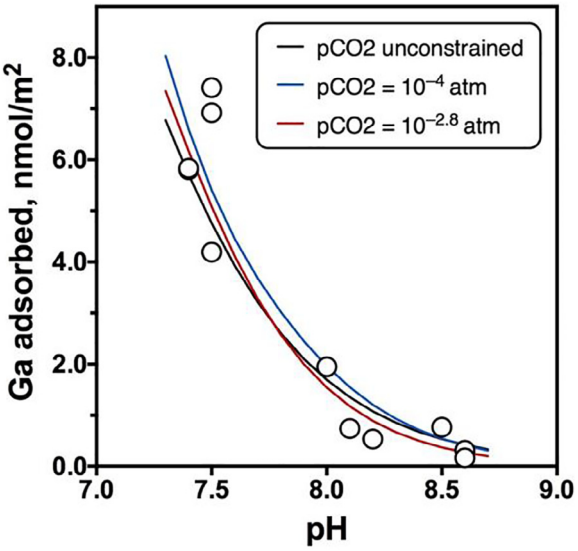

Fig. 2. Measured Ga adsorption on calcite surface as a function of pH (symbols) and SCM predictions (solid lines) for different values of pCO_2. The black line is obtained by changing the CO_2 partial pressure ($5.6 \times 10^{-5} < pCO_2 < 7.3 \times 10^{-3}$ atm), whereas blue and red lines were obtained by fixing pCO_2 at 1.0×10^{-4} and 1.5×10^{-3} atm, respectively. (For interpretation of the references to color in this figure legend, the reader is referred to the web version of this article.)

(expressed in nmol/m^2) was plotted against pH together with the predictions of the SCM model generated in this study for different pCO_2 (three solid curves on the plot) and a calcite/solution ratio of 3.6 g/l. In one case (black solid line) the pH was varied by changing the CO_2 partial pressure while maintaining the fluid at equilibrium with calcite. In contrast, the blue and red curves correspond to the model results obtained by fixing the pCO_2 at 1.0×10^{-4} and 1.5×10^{-3} atm, respectively. These three curves represent plausible fit-lines to the experimental data within the rela-

tively small range of experimental pCO_2, illustrating the good agreement between the data and the SCM model of Ga adsorption proposed here.

3.1.2. Goethite

A summary of the experimental parameters and the corresponding results is reported in Table 4. Five of the runs were sampled a first time 3 days after Ga addition to the suspension (samples G-1, G-6, G-7, G-14 and G-20), and then after 7 days as for all the other experiments. It can be observed that the difference in Ga adsorbed between 3 and 7 days is generally very small (0–2%), suggesting that Ga reached adsorption equilibrium after time periods ≤ 3 days. The dependence of the fraction of adsorbed Ga on goethite concentration is illustrated in Fig. 3A. It can be seen that the extent of Ga adsorption is much weaker at pH = 2.5 than at pH $\geq$ 3.1 and less impacted by the increase of goethite concentration. At pH $\geq$ 3.1 the Ga adsorbed fraction (% Ga adsorbed) increased to 100% when the goethite concentration reached 1 to 7 g/l, whereas the highest percentage of Ga adsorbed at pH = 2.5 was equal to 46% relative to a goethite concentration of 10 g/l (Table 4). This observation is consistent with the results of Persson et al. (2006), who reported 100% of $Ga_{(aq)}$ adsorbed on goethite at 3 < pH < 9.

The SCM we applied with the parameter values listed in Table 2 provided the best fit of the experimental data for Log $K_5 = -1.05 \pm 0.2$. The comparison between measured and calculated Ga adsorbed fractions reported in Table 4 shows that the model is in good agreement with the experimental results, with most of the calculated values differing by 0.1–10% with respect to the experimental measurements. However, the difference between measured and calculated percentage of adsorbed Ga was higher for 6 experiments, varying between 11 and 31%. The measured percentage of Ga adsorbed at the goethite/aqueous solution interface is plotted as a function of pH in Fig. 3B and compared, for three different total Ga concentration values ($[Ga]_{tot}$) representative of our experiments, with the percentage of adsorbed Ga calculated using reaction (5). Despite the variable Ga aqueous concentrations and the different goethite/solution ratios, it can be seen that the calculated curves conform to the experimental data well. The formation of the octahedral Ga surface complex $[>FeOGa(OH)_2^0]$ could thus occur via the interaction with $>FeOH_2^+$ sites of the dominant Ga aqueous species, Ga^{3+} at pH < 4 and $Ga(OH)_4^-$ at pH > 4.5, according to:

$$> FeOH_2^+ + Ga^{3+} + 2H_2O \rightarrow > FeOGa(OH)_2^0 + 4H^+ \quad (7)$$

Table 4
Summary of the Ga adsorption experiments on goethite with the corresponding pH, solid to aqueous solution ratios (Gth/Vol) and initial and final concentration of Ga in solution. Total and adsorbed Ga amounts ($[Ga]_{tot}$ and $[Ga]_{ads}$) are expressed in terms of the goethite surface area [μmol/m^2] of each experiment. The last 2 columns list the adsorbed Ga percentage measured and calculated according to the surface complexation model presented in this study.

Sample no.	pH	Gth/Vol	$[Ga]_{in}$	$[Ga]_{fin}$	$[Ga]_{tot}$	$[Ga]_{ads}$	% Ga adsorbed	
		g/l	ppm	ppm	μmol/m^2	μmol/m^2	Measured	Model
G-1*	2.5	9.9	55.383	30.253	3.45	1.57	45.4	45.7
G-1b	2.5	9.9	55.383	29.905	3.45	1.59	46.0	46.0
G-2	2.5	5.1	58.644	42.154	7.12	2.00	28.1	24.2
G-3	2.5	4.1	58.517	44.394	8.81	2.13	24.1	19.7
G-4	2.5	3.0	5.414	3.772	1.13	0.34	30.3	61.4
G-5	2.5	2.0	5.054	3.745	1.53	0.40	25.9	52.5
G-6*	3.1	9.7	53.571	1.264	3.40	3.32	97.6	92.7
G-6b	3.1	9.7	53.571	1.266	3.40	3.32	97.6	92.7
G-7*	3.1	4.9	52.071	13.515	6.62	4.90	74.0	56.6
G-7b	3.1	4.9	52.071	12.417	6.62	5.04	76.2	58.5
G-8	8.0	1.0	0.101	0.000	0.06	0.06	100.0	99.5
G-9	8.0	6.9	0.103	0.000	0.01	0.01	100.0	99.9
G-10	8.9	1.0	0.605	0.001	0.36	0.36	99.8	96.3
G-11	9.0	0.5	0.604	0.007	0.70	0.69	98.9	91.3
G-12	9.0	0.2	0.609	0.096	1.72	1.45	84.2	80.1
G-13	9.5	0.5	1.247	0.278	1.45	1.12	77.7	74.6
G-14*	10.0	10.3	4.790	0.057	0.29	0.28	98.8	95.3
G-14b	10.0	10.3	4.790	0.044	0.29	0.28	99.1	95.3
G-15	10.0	2.0	4.959	1.098	1.52	1.18	77.9	76.9
G-16	10.0	1.0	4.985	3.005	2.99	1.19	39.7	53.7
G-17	10.0	0.5	4.921	3.969	5.94	1.15	19.3	29.3
G-18	10.0	0.2	5.176	4.086	17.05	3.59	21.1	11.5
G-19	10.1	0.1	5.262	4.492	22.94	3.36	14.6	7.8
G-20*	10.5	10.3	4.960	0.842	0.30	0.25	83.0	84.6
G-20b	10.5	10.3	4.960	0.803	0.30	0.25	83.8	84.7
G-21	10.5	1.0	4.962	3.805	3.00	0.70	23.3	28.6
G-22	10.5	2.0	4.970	2.340	1.51	0.80	52.9	48.6
G-23	10.5	4.0	4.971	1.046	0.77	0.61	79.0	67.5

* This symbol identifies data relative to 3 days of adsorption reaction.

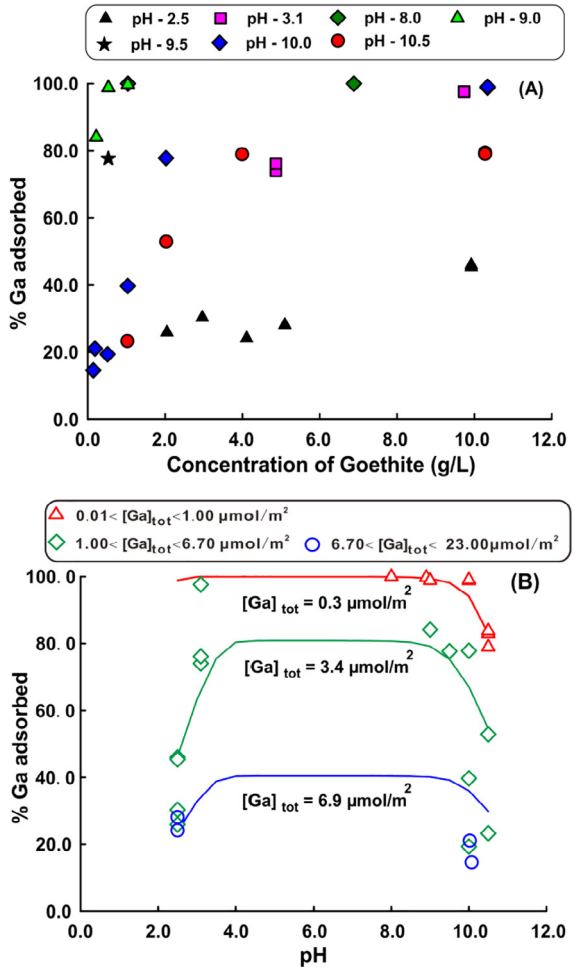

Fig. 3. Percentage of Ga adsorbed as a function of goethite/aqueous solution volume ratio (A) and comparison between measured and calculated percentages of adsorbed Ga as a function of pH in 0.01 M NaCl (B). The three curves shown in (B) represent the predictions of the SCM presented in this study for three different values of surface normalized total Ga concentration ($[Ga]_{tot}$ = 0.3, 3.4 and 6.9 μmol/m^2), which are representative of our experiments (see Table 4).

and

$$> FeOH_2^+ + Ga(OH)_4^- \rightarrow > FeOGa(OH)_2^0 + 2H_2O \quad (8)$$

The values of the equilibrium constants of reactions (7) and (8) can be derived from the calculated value of the equilibrium constant of reaction (5), the protonation constant of goethite functional groups and the value of the fourth Ga hydrolysis constant adopted in this study (Benézéth et al., 1997). The Log K_7 and Log K_8 values thus calculated are equal to −8.52 and 7.14, respectively.

3.2. Ga isotope fractionation during adsorption

3.2.1. Calcite

Our results listed in Table 5 show that in all experiments lighter Ga isotopes were preferentially adsorbed onto the calcite surface, leaving experimental solutions isotopically heavier relative to the initial Ga stock solution ($\delta^{71}Ga_{initial}$ = 1.83‰). The steady-state Ga isotopic composition of solutions was reached within 3 days since the 7-day replicates of the same runs resulted in almost identical Ga isotope compositions within errors.

The Ga isotopic composition of the solutions ($\delta^{71}Ga_{solution}$) is plotted as a function of the fraction of Ga adsorbed on calcite in Fig. 4A. It can be seen that $\delta^{71}Ga_{solution}$ did not exhibit significant variation with the solution pH in the investigated pH range (7.4–8.6). The data reported in Fig. 4B show that the extent of Ga isotope fractionation decreased slightly when the Ga fraction adsorbed on calcite increased, with $\Delta^{71}Ga_{calcite\text{-}solution}$ decreasing from −0.97 ± 0.21‰ to −1.27 ± 0.63‰ when the fraction of Ga removed from solution decreased from ~40% to 10%. Note, however, the large uncertainty affecting the −1.27‰ data due to the small extent of Ga adsorption.

3.2.2. Goethite

The results of the 23 Ga sorption runs performed on goethite are summarized in Table 5 and illustrated by Fig. 5A and B where $\delta^{71}Ga_{solution}$ and $\Delta^{71}Ga_{goethite\text{-}solution}$, respectively, are plotted as a function of the fraction of adsorbed Ga. As for the sorption runs on calcite, the lighter Ga isotopes were preferentially adsorbed at the goethite surface, leaving the solutions isotopically heavier than the initial stock Ga solution ($\delta^{71}Ga_{initial}$ = 1.87‰). It should be noted that for the runs G-1, G-6, G-7, G-14 and G-20 performed at pH 2.5, 3.1, 3.1, 10.0 and 10.5, respectively, the fluid isotopic analyses relative to 3 and 7 days duration yielded the same results within errors (Table 5). Fig. 5A shows that $\delta^{71}Ga_{solution}$ did not exhibit significant variation with solution pH in the large pH range investigated (2.5 ≤ pH ≤ 10.5).

The extent of Ga isotope fractionation between goethite and solution (−0.89‰ ≤ $\Delta^{71}Ga_{goethite\text{-}solution}$ ≤ −0.45‰) was distinctly smaller than that between calcite and solution (−1.27‰ ≤ $\Delta^{71}Ga_{calcite\text{-}solution}$ ≤ −0.97‰) (Table 5 and Fig. 4B and 5B). Furthermore, Ga isotope fractionation between goethite and solution was impacted more than that between calcite and solution by the fraction of Ga adsorbed, the extent of fractionation decreasing by ~0.2‰ when the fraction of Ga removed from solution increased from 20% to near 100% (Fig. 5B).

4. DISCUSSION

4.1. Ga isotope fractionation mechanisms

The results of the experiments with both calcite and goethite are consistent with Ga isotope fractionation during adsorption onto the solid surfaces being the result of an equilibrium isotope effect. As seen in Figs. 4A and 5A, the experimental $\delta^{71}Ga_{solution}$ and $\delta^{71}Ga_{solid}$ data fall on single parallel linear trends and hence are best matched by closed system equilibrium exchange between dissolved and sorbed Ga.

Two main mechanisms could *a priori* account for the Ga isotope fractionations measured in this study: (i) isotope exchange between Ga aqueous species and the Ga complexes formed at the solid surface, and (ii) the preferential

Table 5
Results of Ga isotope fractionation during adsorption on calcite and goethite. The uncertainty of all isotopic measurements (expressed as 2 standard deviation, 2SD) are relative to the 3 replicate measurements carried out for each sample. The isotopic composition of the initial Ga (III) nitrate hydrate ($\delta^{71}Ga_{initial}$) was of 1.83‰ and 1.87‰ for the adsorption experiments conducted with calcite and goethite, respectively.

Adsorbent	Sample no.	Exposure time (days)	pH	Ga adsorbed %	$\delta^{71}Ga_{solution} \pm 2SD$ (‰)	$\delta^{71}Ga_{solid} \pm 2SD$ (‰)	$\triangle^{71}Ga_{solid\text{-}solution} \pm 2SD$ (‰)
Calcite							
	C-1	7	7.4	25.5	2.10 ± 0.05	1.04 ± 0.02	−1.06 ± 0.22
	C-2	7	7.4	25.7	2.08 ± 0.05	1.11 ± 0.02	−0.97 ± 0.21
	C-3	7	7.5	30.3	2.19 ± 0.06	1.00 ± 0.02	−1.19 ± 0.20
	C-4	7	7.5	34.0	2.18 ± 0.06	1.15 ± 0.01	−1.03 ± 0.17
	C-5	7	7.5	41.1	2.25 ± 0.04	1.23 ± 0.01	−1.02 ± 0.12
	C-6	7	8.0	16.1	2.02 ± 0.05	0.84 ± 0.06	−1.18 ± 0.36
	C-7	7	8.1	22.8	2.09 ± 0.05	0.95 ± 0.03	−1.14 ± 0.24
	C-8	7	8.2	26.2	2.10 ± 0.05	1.07 ± 0.02	−1.03 ± 0.22
	C-9	7	8.5	9.5	1.95 ± 0.05	0.68 ± 0.16	−1.27 ± 0.63
	C-10	7	8.6	15.4	2.01 ± 0.04	0.84 ± 0.06	−1.17 ± 0.33
	C-11	7	8.6	16.1	2.02 ± 0.05	0.84 ± 0.06	−1.18 ± 0.39
Goethite							
	G-1*	3	2.5	45.4	2.22 ± 0.04	1.44 ± 0.10	−0.78 ± 0.11
	G-1b	7	2.5	46.0	2.18 ± 0.04	1.50 ± 0.10	−0.68 ± 0.11
	G-2	7	2.5	28.1	2.08 ± 0.05	1.34 ± 0.19	−0.73 ± 0.20
	G-3	7	2.5	24.1	2.04 ± 0.03	1.34 ± 0.20	−0.70 ± 0.20
	G-4	7	2.5	30.3	2.11 ± 0.05	1.32 ± 0.17	−0.80 ± 0.18
	G-5	7	2.5	25.9	2.11 ± 0.04	1.47 ± 0.13	−0.64 ± 0.13
	G-6*	3	3.1	97.6	2.37 ± 0.03	1.86 ± 0.04	−0.52 ± 0.05
	G-6b	7	3.1	97.6	2.37 ± 0.05	1.86 ± 0.04	−0.52 ± 0.07
	G-7*	3	3.1	74.0	2.30 ± 0.05	1.72 ± 0.06	−0.58 ± 0.07
	G-7b	7	3.1	76.2	2.31 ± 0.04	1.73 ± 0.06	−0.58 ± 0.07
	G-12	7	9.0	84.2	2.31 ± 0.03	1.79 ± 0.05	−0.53 ± 0.06
	G-13	7	9.5	77.7	2.29 ± 0.05	1.75 ± 0.05	−0.55 ± 0.07
	G-14*	3	10.0	98.8	2.36 ± 0.03	1.86 ± 0.04	−0.49 ± 0.05
	G-14b	7	10.0	99.1	2.39 ± 0.04	1.87 ± 0.04	−0.52 ± 0.06
	G-15	3	10.0	77.9	2.30 ± 0.04	1.75 ± 0.05	−0.56 ± 0.07
	G-16	7	10.0	39.7	2.16 ± 0.04	1.42 ± 0.12	−0.74 ± 0.13
	G-17	7	10.0	19.3	2.04 ± 0.04	1.16 ± 0.28	−0.89 ± 0.28
	G-18	7	10.0	21.1	2.02 ± 0.05	1.30 ± 0.26	−0.73 ± 0.26
	G-19†	7	10.1	14.6	1.94 ± 0.05	1.48 ± 0.40	−0.45 ± 0.40
	G-20*	3	10.5	83.0	2.33 ± 0.03	1.78 ± 0.05	−0.56 ± 0.06
	G-20b	7	10.5	83.8	2.34 ± 0.02	1.78 ± 0.05	−0.56 ± 0.05
	G-21	3	10.5	23.3	2.04 ± 0.05	1.31 ± 0.23	−0.72 ± 0.23
	G-22	7	10.5	52.9	2.25 ± 0.05	1.53 ± 0.09	−0.72 ± 0.10
	G-23	7	10.5	79.0	2.33 ± 0.05	1.75 ± 0.05	−0.59 ± 0.07

* This symbol identifies data relative to 3 days of adsorption reaction.
† Datapoint not reported in Fig. 5B because of the big uncertainty related to the small adsorption extent.

adsorption of a single type of Ga aqueous species if several Ga species of different isotopic composition co-exist in solution (i.e. $Ga(OH)_2^+$, $Ga(OH)_3^0$, $Ga(OH)_4^-$), which would subsequently shift the isotopic composition of the solution.

4.1.1. Calcite

For this mineral, the preferential adsorption of a single type of Ga aqueous species can be ruled out because at the pH of our experimental solutions (7.4–8.6), $Ga(OH)_4^-$ is the only Ga species present in solution (cf. Table 6 and Benézéth et al., 1997). Thus, the isotope exchange between $Ga(OH)_4^-$ and Ga surface complexes should be responsible for the isotope fractionation reported in the present study.

Ga sorption on calcite can be described by the interaction of $Ga(OH)_4^-$ with the hydrated surface calcium sites, $>CaOH_2^+$, leading to the formation of six- coordinated Ga surface anions, $>Ca\text{-}O\text{-}GaOH(OH_2)_4^+$ sharing one oxygen with a Ca ion at the surface (reaction (6)). Aqueous Ga, therefore, changes its coordination from 4 to 6 when adsorbing on the calcite surface. XAFS observations showed that this coordination change results in an increase of the Ga-O bond length from 1.84 ± 0.01 Å in $Ga(OH)_4^-$ (Pokrovski et al., 2002; Pokrovsky et al., 2004) to 1.94 ± 0.01 Å in the Ga surface complexes (Pokrovsky et al., 2004). Given the general rule that at equilibrium the heavy isotopes of an element would tend to concentrate in the species where that element forms the stiffest (shortest) bonds (Criss, 1999; Schauble, 2004), aqueous $Ga(OH)_4^-$ should therefore be enriched in heavy isotopes (^{71}Ga) compared to the Ga surface complexes. This is exactly what we

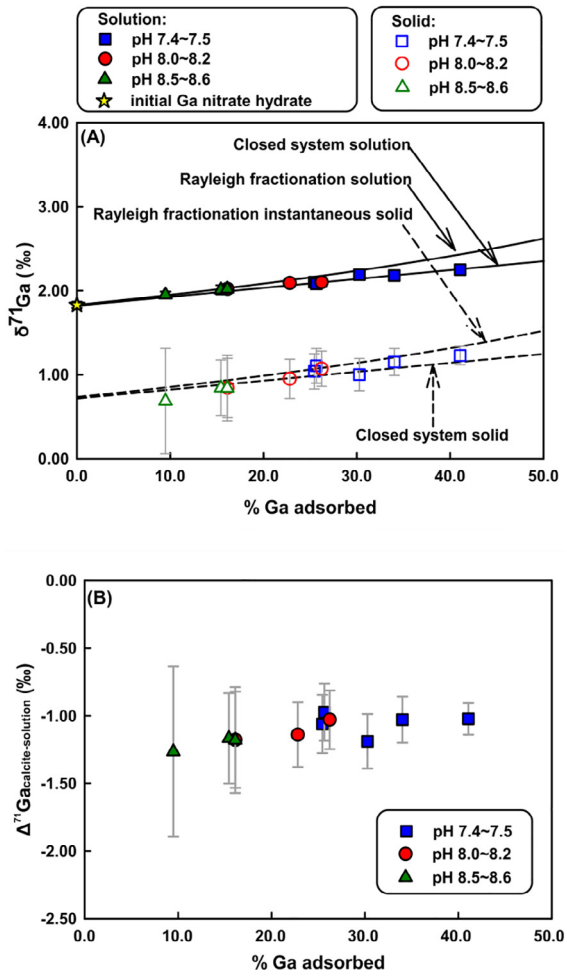

Fig. 4. $\delta^{71}Ga_{solution}$ and $\delta^{71}Ga_{calcite}$ (both measured and inferred) as a function of the fraction of Ga adsorbed by calcite (A), and the extent of Ga isotope fractionation during Ga sorption on calcite ($\triangle^{71}Ga_{calcite\text{-}solution}$) vs. the fraction of Ga adsorbed (B). In (A) the experimental data are compared with the trends predicted for closed system equilibrium and Rayleigh fractionation models calculated using $\alpha_{calcite\text{-}solution} = 0.9989$ (runs C-1, C-3, C-7).

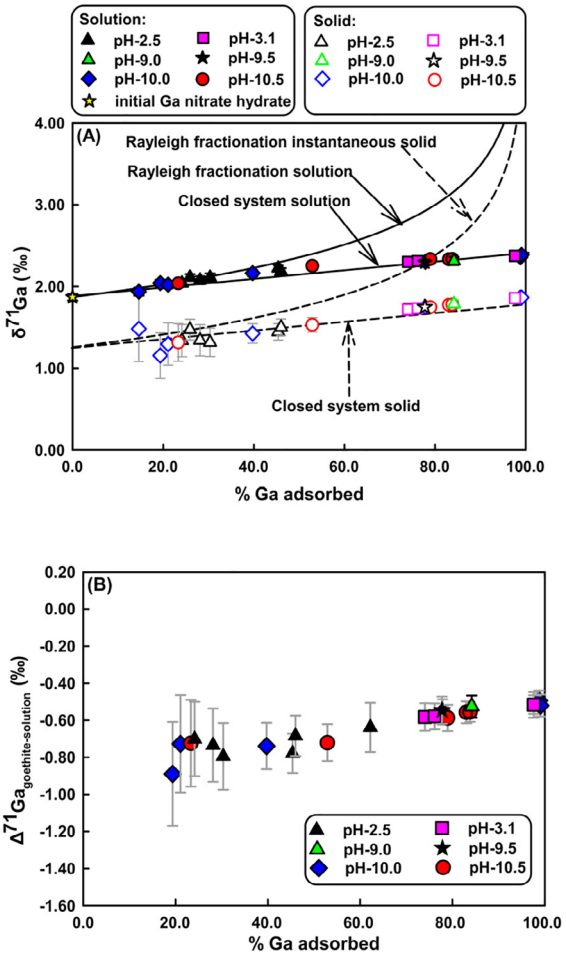

Fig. 5. $\delta^{71}Ga_{solution}$ and $\delta^{71}Ga_{goethite}$ (both measured and inferred) as a function of the fraction of Ga adsorbed by goethite (A), and the extent of Ga isotope fractionation during Ga sorption on goethite ($\triangle^{71}Ga_{goethite\text{-}solution}$) vs. the fraction of Ga adsorbed (B). In (A) the experimental data are compared with the trends predicted for closed system equilibrium and Rayleigh fractionation models calculated using $\alpha_{goethite\text{-}solution} = 0.9993$ (runs G-1, G-1b, G-16, G-22).

observed in all our experiments where Ga sorption on the calcite surface induces an enrichment of the solution in ^{71}Ga.

The observed small decrease of the extent of Ga isotope fractionation with the increasing percentage of adsorbed Ga (Fig. 4B) might be related to the slight changes in the structure of Ga surface complexes with increasing degree of calcite surface coverage by adsorbed Ga. The XAFS study of Pokrovsky et al. (2004) indeed reported that adsorbed Ga at concentrations > 20 nmol/m^2 exhibited second shell contributions arising from Ga-Ga pairs with Ga-Ga distances (~3.05 and ~3.5 Å) very similar to those observed by Pokrovski et al. (2002) for the polymeric Ga hydroxide complexes formed in aqueous solution during Ga^{3+} hydrolysis at $2 < pH < 5$. Since the mean of Ga–O distance in these polymers is distinctly shorter than that in the monomeric $Ga(H_2O)_{6\text{-}4}(OH)_{0\text{–}2}$ species (1.88 ± 0.03 Å vs 1.96 ± 0.01 Å), it can be expected that the extent of isotope fractionation would be slightly reduced for the highest amount of Ga adsorbed at the calcite surface (~10 nmol/m^2) which is indeed shown by our experimental data.

4.1.2. Goethite

The striking feature of the results for goethite is that the solution pH had no discernable effect on the isotope fractionation, although Ga aqueous speciation dramatically differs at pH 2.5/3.1 (only hexacoordinated Ga^{3+} and $GaOH^{2+}$) and pH ≥ 8 (100% $Ga(OH)_4^-$) as shown in Table 6.

Ga adsorption modeling on goethite (this study; Persson et al., 2006) and the XAFS characterization of Ga local structure at the water-goethite interface (Persson et al., 2006) demonstrated the presence of octahedral Ga species, $>FeOGa(OH)_2^0$, sharing two edges and one corner with FeO_6 octahedra at the goethite surface (see Fig. 6). If this

Table 6
Distribution of Ga aqueous species as a function of pH at 25 °C (Benézéth et al., 1997; Persson et al., 2006).

pH	Distribution of Ga aqueous species at 25 °C (I = 0.01, NaCl)	
	Benézéth et al. (1997)	Persson et al. (2006)
2.5	81% Ga^{3+}, 19% $Ga(OH)^{2+}$	95% Ga^{3+}, 5% $Ga(OH)^{2+}$
3.1	48% Ga^{3+}, 50% $Ga(OH)^{2+}$, 2% $Ga(OH)_2^+$	49% Ga^{3+}, 49% $Ga(OH)_3$, 2% $Ga(OH)^{2+}$
≥8.0	100% $Ga(OH)_4^-$	100% $Ga(OH)_4^-$

surface complex was formed by the adsorption of octahedral aqueous Ga (Ga^{3+}/$Ga(OH)^{2+}$) and tetrahedral Ga $(OH)_4^-$ at pH ≤ 3.1 and pH ≥ 8, respectively, a greater extent of Ga isotope fractionation would be expected at pH ≥ 8 because of the Ga coordination (and Ga–O bond length) change between aqueous and sorbed gallium. The lack of effect of pH on Ga isotope fractionation likely indicates that Ga surface complexes are formed by the sorption of $Ga(OH)_4^-$ on the goethite surface at pH 2.5 and 3.1 as well as at pH ≥ 8, although the proportion of $Ga(OH)_4^-$ in the bulk fluid is very small at pH ≤ 3.1 (<0.5% of total aqueous Ga). The preferential adsorption of $Ga(OH)_4^-$ at pH 2.5–3.1 likely results from (i) the difficulty for Ga^{3+} and $Ga(OH)^{2+}$ to get closer to the goethite surface because of the electrostatic repulsion generated by the $>FeOH_2^+$ surface species which account for >99% of goethite surface speciation at pH ≤ 3.1, and (ii) by the increased hydroxide anion concentration in the Stern and diffusive layers near the solid surface due to proton loss by water molecules and anion diffusion to neutralize the goethite solution interface (Tamura et al., 2001; Hiemstra and Van Riemsdijk, 2006). The resulting increase of OH^- concentration (and thus pH) in the 0.1–1 μm thick diffusive layer (Gupta et al., 2007) should favor Ga^{3+} hydrolysis and the formation of $Ga(OH)_4^-$. For example, at pH = 3, an increase in pH of the diffuse layer by only one unit would be enough to increase the proportion of $Ga(OH)_4^-$ from 0.01 to 7%.[1] The change of Ga-O bond length between $Ga(OH)_4^-$ (~1.84 Å) and the surface complexes (~1.96 Å) could thus explain the enrichment in lighter Ga isotope (^{69}Ga) observed both at acid and alkaline pH on the surface of the solid.

The significant reduction of the extent of Ga isotope fractionation with the increasing fraction of Ga removed from solution may be related to the formation of Ga surface polymers with increasing degree of goethite surface coverage by Ga, similar to the case for calcite. The XAFS investigation of Ga local environment at the solution-goethite interface did not allow Persson et al. (2006) to detect second shell contributions arising from Ga-Ga pairs that characterize the presence of polymeric hydroxide complexes or $Ga(OH)_3$ surface precipitates. However, it should be noted that the fraction of goethite surface active sites occupied by Ga was ≤29% in Persson et al. (2006), whereas

[1] Similarly, the borate anion, $B(OH)_4^-$, has been shown to be selectively adsorbed on calcite surfaces to form tetrahedral surface complexes even at 6.5 ≤ pH ≤ 7.7 where this species account for only 0.17–2% of total aqueous boron (Goldberg and Forster, 1991; Goldberg et al., 2000).

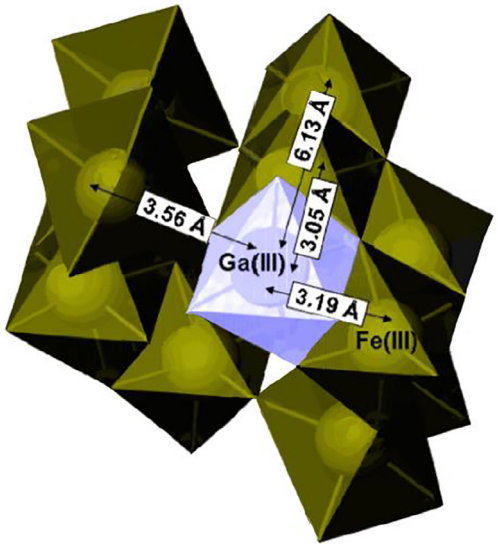

Fig. 6. Schematic structure of the atomic environment of Ga(III) adsorbed onto goethite surface based on EXAFS spectroscopy (modified from Persson et al. (2006)).

it ranged between 0.3% (0.01 μmol/m^2) and 180% (5.04 μmol/m^2) in the present study. Therefore, it is likely that Ga surface polymers and/or $Ga(OH)_3$ surface precipitates were present for the highest Ga surface concentrations of this study (i.e. $[Ga]_{ads}$ > 2 mol/m^2). Because the Ga–O bond lengths in monomeric $>FeOGa(OH)_2^0$ (1.96 Å) would be longer than in Ga surface polymers and $Ga(OH)_3$(s) (~1.88 Å), the latter should be enriched in ^{71}Ga. This would explain the significant reduction of the extent of isotope fractionation observed in this study for the highest degree of Ga surface coverage (>70% of Ga removed from solution, $[Ga]_{ads}$ > 2 mol/m^2).

4.2. Geochemical applications

The results obtained in this study allow for a first evaluation of the degree of Ga isotope fractionation in surficial environments where Ga-bearing solutions interact with calcium carbonates and/or Fe (oxyhydr)oxides. The fractionation factors measured in the present work imply that the infiltration of Ga-bearing fluids through soils or sediments containing carbonates and/or Fe (oxyhydr)oxides should induce enrichments of heavier Ga in the fluid up to 1.25‰ for low water/carbonate ratios or 0.9‰ for low water/Fe (oxyhydr)oxide ratios, respectively. Though Ga isotope fractionation during its co-precipitation with Fe (oxyhydr)oxides has not been investigated at the present

stage, comparable fractionation factors with enrichment of the liquid in heavier isotopes should occur during Ga coprecipitation with iron oxides because in these solids Ga substitutes for Fe in octahedral coordination (Martin et al., 1997). It is thus expected that rivers draining highly weathered magmatic rocks (i.e. in tropical or volcanic arc regions) will be enriched in ^{71}Ga by about 1‰ relative to the unaltered bedrocks. Note that Rayleigh distillation may induce distinctly higher enrichment of heavy Ga in sediment pore waters during the progressive precipitation of Fe-oxides in marine or freshwater sediments, as observed for other isotope systems (i.e. δ^{57}Fe, Rouxel et al., 2008). At the same time, when high amounts of organic matter are available in soils and rivers, the complexation of $Ga(OH)_4^-$ with carboxylic or hydroxyl-carboxylic acids, phenols, di-phenols may lead to an enrichment of heavier Ga in free gallate ions, which is similar to the behavior of other metals (Fe, Cu, Zn, etc.) with organic ligands (Fujii et al., 2014), implying a potential application of Ga isotopes for tracing biological processes.

However, it should be noted that in most rivers with pH > 5, Ga, like Al, is not transported as a true dissolved ionic species but via organic, organo-mineral and mineral colloids or suspended species (e.g., Pokrovsky et al., 2010; Ogawa et al., 2012). Interestingly, as demonstrated by Pokrovsky et al. (2014) for boreal rivers, a significant fraction of Ga can be transferred to the true dissolved pool during estuarine mixing as a result of desorption from colloids and suspended species with progressive increase of pH to that of seawater. Thus, desorption processes in estuaries can lead to significant fluxes to the ocean of true dissolved Ga enriched in ^{71}Ga. On the other hand, according to Orians and Bruland (1988), most dissolved Ga at the surface of the oceans has, like Al, an eolian provenance with the extent of dissolution of Ga from eolian particles close to 50%. Thus, as with estuarine mixing processes, reduction of Ga coordination accompanying this dissolution is likely to enrich the ocean in ^{71}Ga as well as Ga scavenging by solid particles throughout the water column. Vertical profiles of dissolved Ga in the oceans (Orians and Bruland, 1988) show evidence, along with particle scavenging, of a deep water source of Ga from diffusion out of the sediments. This deep supply of dissolved Ga is also likely to be enriched in ^{71}Ga. In the end, one could expect oceanic dissolved Ga to be isotopically heavier than Ga from the continental crust. Consequently, Ga isotopes would be a useful tool for tracing the impact of continental input (through both rivers and atmospheric deposition) on the oceanic biogeochemistry of Ga (and Al).

5. CONCLUDING REMARKS

In this study we carried out a series of experiments aimed at determining Ga isotope fractionation during Ga adsorption on calcite and goethite. Gallium adsorption and corresponding isotopic composition were investigated at 20 °C as a function of pH and for different solid/solution ratios and initial aqueous Ga concentrations. Our results provide the first experimental evidence of significant Ga isotope fractionation during solid-fluid interactions. Adsorption of Ga on calcite and goethite surfaces results in substantial enrichments of the solid surfaces in light Ga isotopes with values of isotope fractionation factors, $\triangle^{71}Ga_{solid\text{-}solution}$, as great as −1.27‰ and −0.89‰ for calcite and goethite, respectively, indicating that Ga isotopes fractionate to a larger extent during adsorption on the surface of calcite than during adsorption on goethite. Our results suggest that the fractionation is mainly triggered by changes of Ga coordination and Ga-O bond length during adsorption of $Ga(OH)_4^-$ onto the solid surface.

Because Ga is present as tetrahedral gallate ions in most natural fluids and forms hexa-coordinated species at the surface of solids, it is likely that the adsorption of Ga by oxides, carbonates or clay minerals could yield significant Ga isotope fractionation between secondary minerals and surficial fluids including seawater. Our study demonstrates the potential of Ga isotopes to increase our understanding of biogeochemical processes at the Earth surface. However, further experimental and theoretical work is needed to quantify Ga isotope fractionation during Ga co-precipitation with secondary minerals (Fe/Mn hydroxides, Fe oxides, carbonates other than calcite, clays) and to further constrain the impact of fluid composition and pH on the extent of Ga isotope fractionation.

ACKNOWLEDGMENTS

Oleg S. Pokrovsky and Thomas D. Bullen are thanked for their helpful comments, constructive suggestions and careful English editing. This work was financially supported by the Natural Science Foundation of China (41625012, U1301231, 41561134017, U1612442), the State Key Laboratory of Environmental Geochemistry, IGCAS (SKLEG2016001) and the GET Laboratory (CNRS-Toulouse University). This is IPGP contribution No. 3905.

APPENDIX A. SUPPLEMENTARY MATERIAL

Supplementary data associated with this article can be found, in the online version, at https://doi.org/10.1016/j.gca.2017.12.008.

REFERENCES

Balistrieri L. S., Borrok D. M., Wanty R. B. and Ridley W. I. (2008) Fractionation of Cu and Zn isotopes during adsorption onto amorphous Fe (III) oxyhydroxide: experimental mixing of acid rock drainage and ambient river water. *Geochim. Cosmochim. Acta* **72**, 311–328.

Barling J. and Anbar A. (2004) Molybdenum isotope fractionation during adsorption by manganese oxides. *Earth Planet. Sci. Lett.* **217**, 315–329.

Barrón V. and Torrent J. (1996) Surface hydroxyl configuration of various crystal faces of hematite and goethite. *J. Colloid Interf. Sci.* **177**, 407–410.

Benézéth P., Diakonov I. I., Pokrovski G. S., Dandurand J.-L., Schott J. and Khodakovsky I. L. (1997) Gallium speciation in aqueous solution. Experimental study and modelling: Part 2. Solubility of α-GaOOH in acidic solutions from 150 to 250 C and hydrolysis constants of gallium (III) to 300 C. *Geochim. Cosmochim. Acta* **61**, 1345–1357.

Berner R. A. (1997) The rise of plants and their effect on weathering and atmospheric CO_2. *Science* **276**, 544–546.

Burton J., Culkin F. and Riley J. (1959) The abundances of gallium and germanium in terrestrial materials. *Geochim. Cosmochim. Acta* **16**, 151–180.

Cornell R. M. and Schwertmann U. (2004) *The Iron Oxides: Structures, Properties, Reactions, Occurrences and Uses*, 2nd ed. Wiley-VCH, p. 670.

Criss R. E. (1999) *Principles of Stable Isotope Distribution*. Oxford University Press, p. 264.

De Laeter J. R. (1972) The isotopic composition and elemental abundance of gallium in meteorites and in terrestrial samples. *Geochim. Cosmochim. Acta* **36**, 735–743.

Delstanche S., Opfergelt S., Cardinal D., Elsass F., André L. and Delvaux B. (2009) Silicon isotopic fractionation during adsorption of aqueous monosilicic acid onto iron oxide. *Geochim. Cosmochim. Acta* **73**, 923–934.

Doherty (2010) *PEST. Model-independent parameter estimation. User Manual*, 5th ed. Watermark Numerical Computing, Web: http://www.pesthomepage.org.

Fujii T., Moynier F., Blichert-Toft J. and Albarède F. (2014) Density functional theory estimation of isotope fractionation of Fe, Ni, Cu, and Zn among species relevant to geochemical and biological environments. *Geochim. Cosmochim. Acta* **140**, 553–576.

Gaillardet J., Dupré B., Louvat P. and Allegre C. (1999) Global silicate weathering and CO_2 consumption rates deduced from the chemistry of large rivers. *Chem. Geol.* **159**, 3–30.

Gaillardet J., Viers J. and Dupré B. (2003) Trace elements in river waters. *Treatise Geochem.* **5**, 225–272.

Galy A. and France-Lanord C. (1999) Weathering processes in the Ganges-Brahmaputra basin and the riverine alkalinity budget. *Chem. Geol.* **159**, 31–60.

Goldberg S. and Forster E. H. (1991) Boron sorption on calcareous soils and reference calcites. *Soil Sci.* **152**, 304–310.

Goldberg S., Lesch S. M. and Suarez D. L. (2000) Predicting boron adsorption by soils using soil chemical parameters in the constant capacitance model. *Soil Sci. Soc. Am. J.* **64**, 1356–1363.

Goldschmidt V. M. (1954) *Geochemistry*. LWW.

Gottardi G., Burton J. and Culkin F. (1978) Gallium. *Handbook Geochemistry* **2**, 3.

Gupta A. K., Coelo D. and Adler P. M. (2007) Influence of the Sterner layer on elektokinetic phenomena in porous media. *J. Colloid Interf. Sci.* **316**, 140–159.

Gussone N., Schmitt A. D., Heuser A., Wombacher F., Dietzel M., Tipper E. and Schiller M. (2016) *Calcium Stable Isotope Geochemistry*. Springer Ed., p. 260.

Gustafsson J. P. (2012). Visual MINTEQ (v3.1). A Windows version of MINTEQA2. http://vminteq.lwr.kth.se/>.

Hiemstra T. and Van Riemsdijk W. H. (2006) On the relationship between charge distribution, surface hydration, and the structure of interface of metal hydroxides. *J. Colloid Interf. Sci.* **301**, 1–18.

Hilton R. G., Galy A., Hovius N., Horng M.-J. and Chen H. (2011) Efficient transport of fossil organic carbon to the ocean by steep mountain rivers: an orogenic carbon sequestration mechanism. *Geology* **39**, 71–74.

Hindshaw R. S., Reynolds B. C., Wiederhold J. G., Kretzschmar R. and Bourdon B. (2011) Calcium isotopes in a proglacial weathering environment: Damma glacier, Switzerland. *Geochim. Cosmochim. Acta* **75**, 106–118.

Hydes D. (1979) Aluminum in seawater: control by inorganic processes. *Science* **205**, 1260–1262.

Hydes D. (1983) Distribution of aluminium in waters of the North East Atlantic 25 N to 35 N. *Geochim. Cosmochim. Acta* **47**, 967–973.

Hydes D. and Liss P. (1977) The behaviour of dissolved aluminium in estuarine and coastal waters. *Estuar. Coast. Mar. Sci.* **5**, 755–769.

Kato C., Moynier F., Foriel J., Teng F.-Z. and Puchtel I. S. (2017) The gallium isotopic composition of the bulk silicate Earth. *Chem. Geol.* **448**, 164–172.

Lemarchand E., Schott J. and Gaillardet J. (2005) Boron isotopic fractionation related to boron sorption on humic acid and the structure of surface complexes formed. *Geochim. Cosmochim. Acta* **69**, 3519–3533.

Lemarchand E., Schott J. and Gaillardet J. (2007) How surface complexes impact boron isotope fractionation: evidence from Fe and Mn oxides sorption experiments. *Earth Planet. Sci. Lett. Sci. Lett.* **260**, 277–296.

Lövgren L., Sjöberg S. and Schindler P. W. (1990) Acid/base reactions and Al (III) complexation at the surface of goethite. *Geochim. Cosmochim. Acta* **54**, 1301–1306.

Lumsdon D. O. and Evans L. J. (1994) Surface complexation model parameters for goethite (α-FeOOH). *J. Colloid Interf. Sci.* **164**, 119–125.

Martell A. E. and Hancock R. D. (2013) *Metal complexes in aqueous solutions*. Springer Science & Business Media.

Martin F., Ildefonse P., Hazemann J., Mathe P., Noack Y., Grauby O., Beziat D. and De Parseval P. (1997) Gallium crystal chemistry in synthetic goethites. *Le Journal de Physique IV* **7**, C2-821-C822-822.

Mason T. F., Weiss D. J., Horstwood M., Parrish R. R., Russell S. S., Mullane E. and Coles B. J. (2004) High-precision Cu and Zn isotope analysis by plasma source mass spectrometry Part 2. Correcting for mass discrimination effects. *J. Anal. Atom. Spectrom.* **19**, 218–226.

Measures C. and Edmond J. (1988) Aluminium as a tracer of the deep outflow from the Mediterranean. *J. Geophys. Res.-Oceans* **93**, 591–595.

Nilsson N., Lövgren L. and Sjöberg S. (1992) Phosphate complexation at the surface of goethite. *Chem. Spec. Bioavailab.* **4**, 121–130.

Oelze M., von Blanckenburg F., Hoellen D., Dietzel M. and Bouchez J. (2014) Si stable isotope fractionation during adsorption and the competition between kinetic and equilibrium isotope fractionation: implications for weathering systems. *Chem. Geol.* **380**, 161–171.

Ogawa Y., Ishiyama D., Shikazono N., Iwane K., Kajiwara M. and Tsuchiya N. (2012) The role of hydrous ferric oxide precipitation in the fractionation of arsenic, gallium, and indium during the neutralization of acidic hot spring water by river water in the Tama River watershed, Japan. *Geochim. Cosmochim. Acta* **86**, 367–383.

Opfergelt S., Georg R. B., Delvaux B., Cabidoche Y. M., Burton K. W. and Halliday A. N. (2012) Mechanisms of magnesium isotope fractionation in volcanic soil weathering sequences, Guadeloupe. *Earth Planet. Sci. Lett.* **341**, 176–185.

Orians K. J. and Bruland K. W. (1988) The marine geochemistry of dissolved gallium: a comparison with dissolved aluminum. *Geochim. Cosmochim. Acta* **52**, 2955–2962.

Pearson R. (1963) Soft and hard acids and bases. *J. Am. Chem. Soc.* **12**, 3538–3546.

Persson P., Zivkovic K. and Sjöberg S. (2006) Quantitative adsorption and local structures of Gallium (III) at the water-alpha-FeOOH interface. *Langmuir* **22**, 2096–2104.

Pivovarov S. (1997) Surface structure and site density of the oxide-solution interface. *J. Colloid Interf. Sci.* **196**, 321–323.

Pokrovski G. S., Schott J., Hazemann J.-L., Farges F. and Pokrovsky O. S. (2002) An X-ray absorption fine structure and nuclear magnetic resonance spectroscopy study of gallium–

silica complexes in aqueous solution. *Geochim. Cosmochim. Acta* **66**, 4203–4222.

Pokrovsky O. S. and Schott J. (2002) Surface chemistry and dissolution kinetics of divalent metal carbonates. *Environ. Sci. Technol.* **36**, 426–432.

Pokrovsky O. S., Schott J. and Thomas F. (1999) Processes at the magnesium-bearing carbonate/solution interface. 1. A surface speciation model of magnesite. *Geochim. Cosmochim. Acta* **63**, 863–880.

Pokrovsky O. S., Pokrovski G. and Schott J. (2004) Gallium (III) adsorption on carbonates and oxides: X-ray absorption fine structure spectroscopy study and surface complexation modeling. *J. Colloid Interf. Sci.* **279**, 314–325.

Pokrovsky O. S., Pokrovski G., Schott J. and Galy A. (2006) Experimental study of germanium adsorption on goethite and germanium coprecipitation with iron hydroxide: X-ray absorption fine structure and macroscopic characterization. *Geochim. Cosmochim. Acta* **70**, 3325–3341.

Pokrovsky O. S., Mielczarski J. A., Barres O. and Schott J. (2000) Surface speciation models of calcite and dolomite/aqueous solution interfaces and their spectroscopic evaluation. *Langmuir* **16**, 2677–2688.

Pokrovsky O. S., Viers J., Shirokova L., Shevchenko V., Filipov A. and Dupré B. (2010) Dissolved, suspended, and colloidal fluxes of organic carbon, major and trace elements in the Severnaya Dvina River and its tributary. *Chem. Geol.* **273**, 136–149.

Pokrovsky O. S., Galy A., Schott J., Pokrovski G. S. and Mantoura S. (2014) Germanium isotope fractionation during Ge adsorption on goethite and its coprecipitation with Fe oxy (hydr) oxides. *Geochim. Cosmochim. Acta* **131**, 138–149.

Rayleigh L. (1902) On the distillation of binary mixtures. *Phil. Mag. Sci.* **6**(4), 521–537.

Rouxel O., Sholkovitz E., Charette M. and Edwards K. J. (2008) Iron isotope fractionation in subterranean estuaries. *Geochim. Cosmochim. Acta* **72**, 3413–3430.

Schauble E. A. (2004) Applying stable isotope fractionation theory to new systems. *Rev. Mineral. Geochem.* **55**, 65–111.

Schott J., Mavromatis V., Fujii T., Pearce C. R. and Oelkers E. H. (2016) The control of carbonate mineral Mg isotope composition by aqueous speciation: theoretical and experimental modeling. *Chem. Geol.* **445**, 120–134.

Shiller A. M. (1988) Enrichment of dissolved gallium relative to aluminum in natural waters. *Geochim. Cosmochim. Acta* **52**, 1879–1882.

Shiller A. M. and Frilot D. M. (1996) The geochemistry of gallium relative to aluminum in Californian streams. *Geochim. Cosmochim. Acta* **60**, 1323–1328.

Tagirov B. and Schott J. (2001) Aluminum speciation in crustal fluids revisited. *Geochim. Cosmochim. Acta* **65**, 3965–3992.

Tamura H., Mita K., Tanaka A. and Makoto I. (2001) Mechanism of hydroxylation of metal oxide surfaces. *J. Colloid Interf. Sci.* **243**, 202–207.

Teng F. Z., Li W. Y., Rudnick R. L. and Gardner L. R. (2010) Contrasting lithium and magnesium isotope fractionation during continental weathering. *Earth Planet. Sci. Lett.* **300**, 63–71.

Tipper E. T., Bickle M. J., Galy A., West A. J., Pomiès C. and Chapman H. J. (2006) The short term climatic sensitivity of carbonate and silicate weathering fluxes: insight from seasonal variations in river chemistry. *Geochim. Cosmochim. Acta* **70**, 2737–2754.

Van Cappellen P., Charlet L., Stumm W. and Wersin P. (1993) A surface speciation model of the carbonate mineral-aqueous solution interface. *Geochim. Cosmochim. Acta* **57**, 3505–3518.

Vance D., Teagle D. A. and Foster G. L. (2009) Variable Quaternary chemical weathering fluxes and imbalances in marine geochemical budgets. *Nature* **458**, 493–496.

Wedepohl K. H. (1995) The composition of the continental crust. *Geochim. Cosmochim. Acta* **59**, 1217–1232.

Wood S. A. and Samson I. M. (2006) The aqueous geochemistry of gallium, germanium, indium and scandium. *Ore Geol. Rev.* **28**, 57–102.

Yang L. and Meija J. (2010) Resolving the germanium atomic weight disparity using multicollector ICPMS. *Anal. Chem.* **82**, 4188–4193.

Yuan W., Chen J. B., Birck J.-L., Yin Z. Y., Yuan S. L., Cai H. M., Wang Z. W., Huang Q. and Wang Z. H. (2016) Precise analysis of gallium isotopic composition by MC-ICP-MS. *Anal. Chem.* **88**, 9606–9613.

Zhang T., Zhou L., Yang L., Wang Q., Feng L.-P. and Liu Y.-S. (2016) High precision measurements of gallium isotopic compositions in geological materials by MC-ICP-MS. *J. Anal. Atom. Spectrom.* **31**, 1673–1679.

Associate editor: Caroline L. Peacock